

EFFICIENT ASSIMILATION OF RADAR DATA AT HIGH RESOLUTION
FOR SHORT-RANGE NUMERICAL WEATHER PREDICTION

K. Brewster¹, M. Hu^{1,2}, M. Xue^{1,2}, and J. Gao¹

¹Center for Analysis and Prediction of Storms and

²School of Meteorology, University of Oklahoma, Norman, OK 73019, USA

1 INTRODUCTION

High-resolution cloud-resolving numerical weather prediction (NWP) models have the potential to improve the short-term prediction of high-impact weather beyond extrapolation. The development of high-resolution non-hydrostatic models, the rapid increase of computer power, and the availability of full-precision radar data in real-time are making the explicit prediction of thunderstorms a reality (e.g., Droegemeier, 1990, Lilly 1990, Droegemeier 1997, Xue et al. 2003, X03 hereafter).

To be successful, a high-resolution short-term prediction system must assimilate Doppler radar data including radial velocity and reflectivity, and combine that information with data from satellites, surface stations, and other meso- and micro-scale sensor networks. Such an assimilation system must produce a balanced state that can provide a relatively noise-free forward forecast and also contain the hydrometeors and latent heating effects that eliminate the need for spinning up mesoscale and storm-scale motions during the initial period of forecast.

The Center for Analysis and Prediction of Storms (CAPS) and School of Meteorology (OU SoM) at the University of Oklahoma have been working on the storm scale assimilation problem since the inception of CAPS in 1989. CAPS has produced real-time forecasts of convective weather for various field projects dating back to the VORTEX in 1994 and 1995 (Droegemeier et al. 1996a; Xue et al. 1996a). Rather successful real time forecasts using a relocatable 3 km grid were conducted in the spring of 1996 (Droegemeier et al. 1996b; Xue et al. 1996b) and in following years (e.g., Carpenter et al. 1999).

Current areas of research include the use of Ensemble Kalman Filter (EnKF) techniques to assimilate radar data (Tong and Xue 2005, Xue et al. 2005a,b) and 4DVAR methods (Ren and Xue, 2004), as well as the development of 3DVAR for storm-scale analysis and physical initialization of hydrometeors. While the computations for some of EnKF and 4DVAR work are done in research mode, a system using a 3DVAR wind analysis combined with a physical cloud and hydrometeor initialization and latent heat adjustment scheme is built to support real-time forecasting, for limited-area domains on a single multi-processor workstation, or for large high-resolution domains on supercomputing clusters. It is this system that is the subject of this paper, though the radar and satellite processing procedures described here are also utilized with the other techniques being developed and tested.

The system consists of four principal components, 1) programs to remap and super-ob the radar and satellite data to the analysis grid, 2) a 3DVAR system for analysing all data except for clouds and precipitation, 3) a cloud-and-hydrometeor analysis which also applies diabatic adjustments to the temperature fields, and 4) a non-hydrostatic forecast model. The assimilation can be performed as a sequence of intermittent cycles. Also, an incremental analysis update procedure (IAU, Bloom 1996) can be employed in which the analysis increments are applied to the model state gradually over a period of time. Due to the short life cycles of thunderstorms, the IAU assimilation window commonly used is on the order of 10 minutes (Brewster 2002). The assimilation component is an option within the CAPS Advanced Regional Prediction System (Xue et al., 1995; 2003). A conversion program is also available to transform the analyses into a form suitable for initializing the Weather Research and Forecast (WRF) model.

2 CLOUD AND HYDROMETEOR ANALYSIS

Variational assimilation of indirect measurements of cloud and precipitation variables has proven challenging because the microphysical models are

¹ Corresponding author address: Keith Brewster, CAPS, Univ. of Oklahoma, Norman, OK 73019
kbrewster@ou.edu

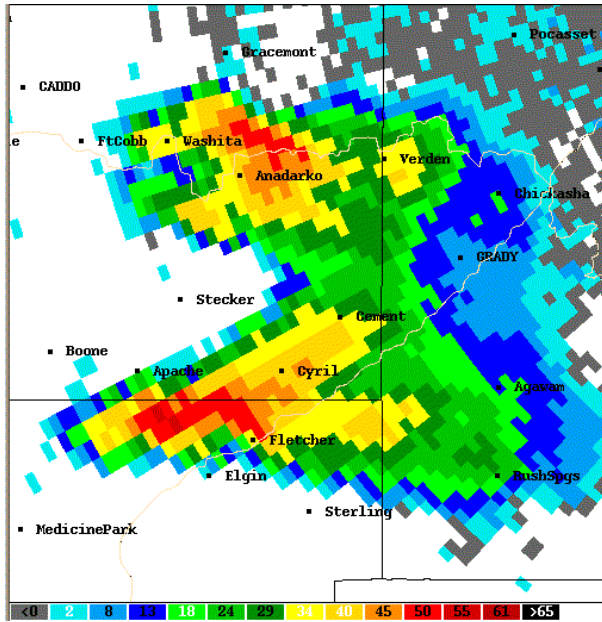


Fig. 1. Raw radar reflectivity (dBZ) display for 3 May 1999 2200 UTC, Oklahoma City radar, KTLX, 0.5 degree elevation angle.

very non-linear and contain complex conditional branching which can result in multi-minima in a variational cost function and inefficient descent. In the case of 3DVAR, insufficient information is available for updating multiple microphysical species from reflectivity observation. The cloud analysis procedure in our system uses physical rules to obtain reasonable cloud and hydrometeor fields from the radar, satellite and surface data. The system first processes each radar volume scan and each satellite data file. Then the data are combined with the surface data to produce the cloud and precipitating hydrometeor fields.

2.1 Radar Data Processing

The data are first quality-controlled for anomalous propagation artifacts by testing for high vertical gradients of reflectivity, reflectivity texture, and very low wind speeds, as guided by statistics presented in Kessinger et al. (1999) and our own tuning.

The radial velocities are unfolded in a three-step process. First, radial velocities are transformed to increments from the mean wind, where the mean wind profile is provided by an average of data points in the background wind field surrounding the radar. This helps to remove the vertical shear of the mean wind shear that can mislead shear-checking algorithms and helps to identify folded velocities in more isolated patches. Next, a hori-

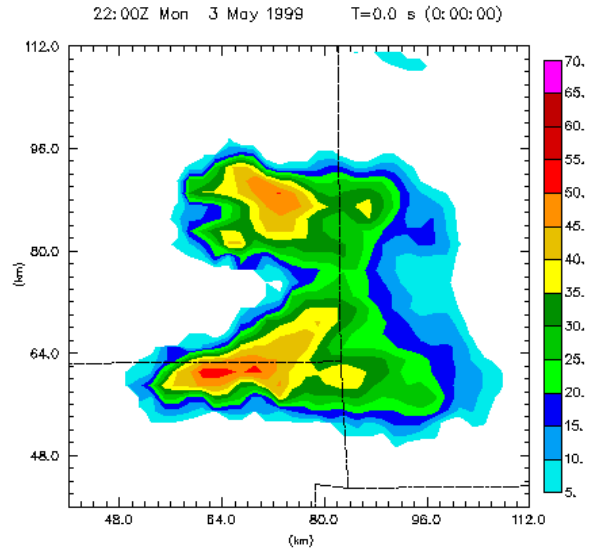


Fig. 2. KTLX radar reflectivity (dBZ) as depicted in Fig. 1, but remapped to Cartesian grid at 3-km resolution

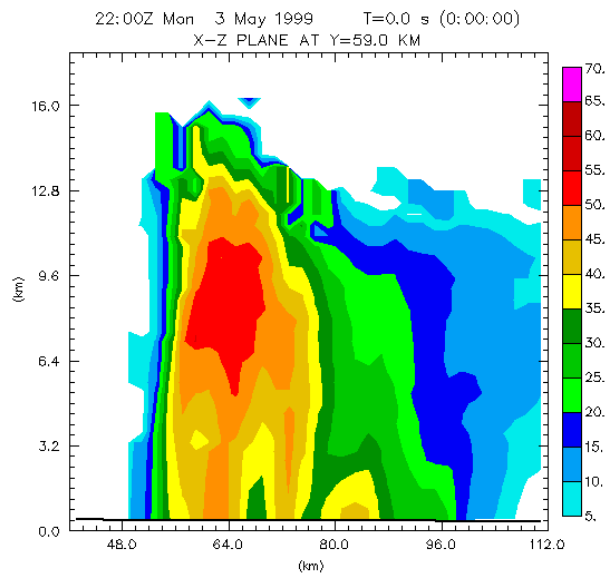


Fig 1c Vertical cross-section along $y=59$ km of KTLX radar reflectivity remapped to terrain-following model grid.

zontal consistency check is applied by measuring gate-to-gate shear, beginning with the radials having azimuths most perpendicular to the mean wind. Finally, local least-squares surface fitting is used to help diagnose folding in areas where the algorithm was uncertain in the previous step.

The data from each radar are then brought to a common resolution by remapping the polar-coordinate data to the Cartesian terrain-following model grid. This is accomplished by a least-

squares fit to a local polynomial function that is quadratic in the horizontal and linear in the vertical:

$$A = a_0 + a_1x + a_2x^2 + a_3y + a_4y^2 + a_5xy + a_6z,$$

where A is the analyzed variable and a_i are the polynomial coefficients. To avoid any unnatural extrapolation, the result is constrained within the range of data that go into the least squares calculation. At grid resolutions of one to few kilometers, this process performs thinning of radar data by smoothing at close range from the radar, but acts as an interpolator at longer ranges from the radar. The same remapping method is applied to the reflectivity and radial velocity. Figures 1-3 serve to demonstrate the remapping for a supercell storm case showing the input data, a remapped horizontal and vertical slice, respectively.

The remapping program can also produce a velocity azimuth display (VAD) wind profile analysis from the quality-controlled winds, and the resultant radar wind profile can be used as an input in the analysis of the large scale wind field.

The software currently supports the NEXRAD Level-II and NIDS (Level-III) and Terminal Doppler Weather Radar (TDWR) operational radar data formats.

The radar processing is done independently for each radar volume which makes it inherently parallel. The processing of data from multiple radars can be distributed to different processors of a cluster.

2.2 Satellite Data Processing

Visible and 11-micron infrared geostationary satellite data in McIDAS AREA file format (such as those from the GOES satellites) are processed by averaging the pixel data onto the Cartesian model grid. Incident brightness corrections are applied for sun angle to compute an albedo. Calibration constants are applied following the methods of the Advanced Satellite Products Team at NOAA/NESDIS to produce cloud top temperature data from the infrared data using calibration coefficient files from NESDIS.

2.3 Cloud Analysis

The initial foundation of the cloud analysis system was the original LAPS cloud analysis (Albers et al. 1995), with adaptation to a general terrain-following grid and other enhancements as described by Zhang et al. (1998) and further refinements by Brewster (2002) and Hu et al. (2005a). Rules are used to combine the surface observations of cloud layers with satellite measurements of cloud top information, radar data, and thermodynamic information from the 3-dimensional analysis of state variables.

2.4 Assigning Hydrometeor Mixing Ratios

The radar reflectivity and thermodynamics are used to solve for the hydrometeor mixing ratios. Because the radar reflectivity is generally a function of drop diameter raised to the sixth power and the water content is a function of diameter cubed, some assumptions must be made about drop size distribution (DSD). The present system uses relationships developed by Smith et al. (1975) based on a Marshall-Palmer DSD, with slight differences introduced in Tong and Xue (2005). Similar formulae are also used by Ferrier (1994). The analysed temperature is used in the scheme in the diagnosis of precipitation species. Direct replacement of the background hydrometeors is done in areas where observed reflectivity is greater than a prescribed threshold (typically 10-20 dBZ). Precipitation is removed from the background in areas within the radar volume coverage and having reflectivity less than the precipitation threshold.

A sample output cross-section of the precipitation hydrometeors, rain water, snow and hail corresponding to the reflectivity cross-section in Figure 3 is shown in Figure 4.

2.5 Latent Heat Adjustment

An important aspect to building and maintaining thunderstorm updrafts in a non-hydrostatic model is the inclusion of the effect of latent heat release due to condensation processes in the updraft regions. The system introduces latent heat adjustment in areas that have analyzed clouds and positive vertical motion. Although, in general, the analysis of vertical velocity itself is a challenge, the introduction of the Doppler radial velocity via the 3DVAR analysis lends more credibility to the

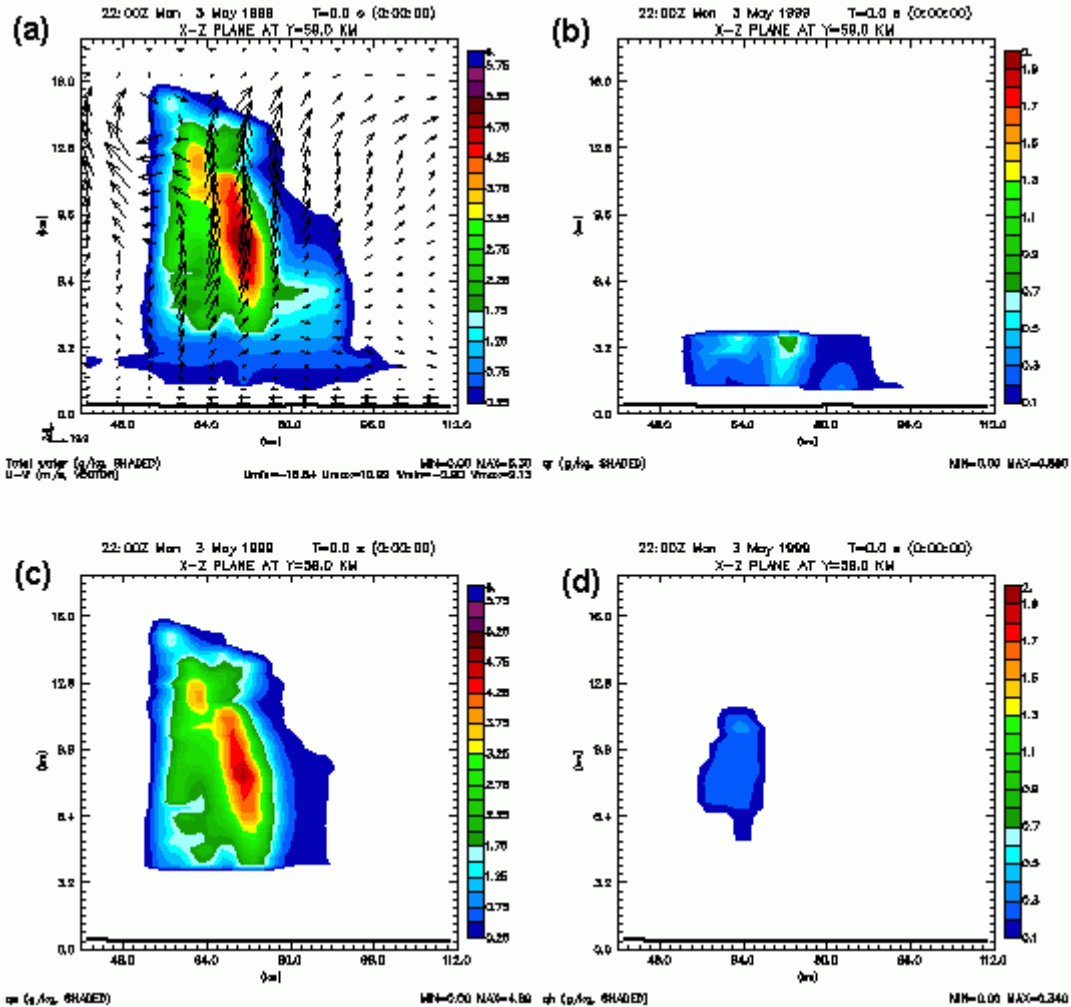


Fig 4. Vertical cross section of analyzed hydrometeors along $y=59$ km for 3 May 1999 2200 UTC, a) winds and total water (g/kg), b) rain water mixing ratio (g/kg), c) snow mixing ratio (g/kg) and d) hail mixing ratio (g/kg).

analyzed vertical motions. We believe that the 3DVAR can provide reliable estimates of the sign of the vertical velocity even though the magnitude tends to be under-estimated.

A moist adiabatic ascent from the analyzed cloudbase with entrainment is calculated and any excess in this temperature over the analyzed temperature is then added to the analyzed value. The same ascent profile is used to derive the mixing ratio of cloud water and cloud ice which replace the background variables. Because of scavenging by precipitating hydrometeors, the cloud water and ice are reduced to 10 percent of the analyzed mixing ratio where precipitating hydrometeors are also diagnosed. This is a heuristic adjustment based on testing for a few

cases, and more work is needed to find the most accurate accounting for the scavenging.

3 3DVAR Analysis

The 3DVAR analysis method developed for the ARPS model, including dynamic constraints appropriate for storm-scale analysis, is documented in Gao et al. (1999, 2004). The analysis variables contain the three wind components (u , v , and w), potential temperature (θ), pressure (p) and water vapor mixing ratio (q_v). In the current system, the cross-correlations between variables are not included in the background error covariance. The background error correlations for single control variables are modeled by a recursive spatial filter. The observation errors are assumed to be

uncorrelated, hence observation error covariance is a diagonal matrix, and its diagonal elements are specified according to the estimated observation errors.

One unique feature of the ARPS 3DVAR is that multiple analysis passes can be used to analyze different data types with different filter scales to account for the variations in the observation spacing among different data sources.

3.1 Analysis Method

The ARPS 3DVAR uses the incremental form of the variational problem. As described in Gao et al. (2004), the classic variational form is employed:

$$J(\mathbf{x}) = \frac{1}{2}(\mathbf{x} - \mathbf{x}^b)^T \mathbf{B}^{-1}(\mathbf{x} - \mathbf{x}^b) + \frac{1}{2}[H(\mathbf{x}) - \mathbf{y}^o]^T \mathbf{R}^{-1}[H(\mathbf{x}) - \mathbf{y}^o] + J_c(\mathbf{x})$$

Where J is the cost function to be minimized, \mathbf{x} is the analysis state vector (consisting of the u , v , and w wind components, pressure, potential temperature and water vapor). \mathbf{x}^b is the background state, either from a large-scale model or a previous run of the storm-scale model. \mathbf{B} is the background error covariance matrix. H is the forward model that converts from the state variables to the observed variables. J_c is a dynamic constraint term, as described in Section 3.2. Then an incremental form is introduced

$$J_{inc}(\mathbf{v}) = \frac{1}{2}\mathbf{v}^T \mathbf{v} + \frac{1}{2}(\mathbf{H}\mathbf{B}^{1/2}\mathbf{v} - \mathbf{d})^T \mathbf{R}^{-1}(\mathbf{H}\mathbf{B}^{1/2}\mathbf{v} - \mathbf{d}) + J_c(\mathbf{v})$$

Where \mathbf{v} is the incremental form of \mathbf{x} from $\sqrt{\mathbf{B}}\mathbf{v} = (\mathbf{x} - \mathbf{x}^b)$, \mathbf{H} is the linearized version of H and $\mathbf{d} \equiv \mathbf{y}^o - H(\mathbf{x}^b)$.

The projection of model data to the radial velocity is accomplished according to

$$V_r = \frac{(X - X_{radar})u + (Y - Y_{radar})v + (Z - Z_{radar})w}{r}$$

where u , v and w are the wind components in Cartesian coordinates (X, Y, Z) ; and $(X_{radar}, Y_{radar}, Z_{radar})$ are the coordinates of radar; r

is the distance from the radar location to the observation points of radial velocity.

Although this is a simplified form of the local slope of the radar beam, we do use the 4/3rds earth radius approximation within the radar remapping scheme to properly locate the radar data in space. Furthermore we provide an option for a first-order correction to the ray path to account for the deviations of the temperature and moisture gradient from the standard atmosphere. A preliminary examination of the errors introduced by such approximation shows that the sensitivity of the beam position to the radar ray path equation is largely confined to elevation angles below 1.0 degree and for special moisture and temperature profiles (Gao et al. 2005).

3.2 Divergence Constraint

In the ARPS 3DVAR, the following weak anelastic mass continuity constraint is imposed on the analyzed wind field:

$$J_c = \frac{1}{2}\lambda_c^2 D^2$$

where λ_c is a weighting coefficient that controls the relative importance of this penalty term in the cost function. D has the form of

$$D = \alpha \left(\frac{\partial \bar{\rho} u}{\partial x} + \frac{\partial \bar{\rho} v}{\partial y} \right) + \beta \frac{\partial \bar{\rho} w}{\partial z}$$

where $\bar{\rho}$ is the mean air density at given height levels, α and β are weighting coefficients.

It was found through experience with the true 3-d divergence constraint ($\alpha=\beta=1$) that the small values of dz in the discretized model relative to dx and dy were causing most of the adjustment in the winds to go into the vertical velocity, with very little effect on the horizontal winds. Experimentation by Hu et al. (2005b) found that the use of the weighting coefficients, with $\lambda_c=1000$, $\alpha=1$ and $\beta=0$, results in a more realistic 3-d wind field and better predictions of the rotational wind within the storms. This combination of weights is the same as imposing a penalty for 2-d divergence. This is effective for this purpose because it is a weak constraint, the 2-d divergence is not forced to be exactly zero, which would not be desired, because we expect storms to have significant convergence and divergence near updrafts and downdrafts. Similar analysis and forecast results were found for the case studied when $\alpha = 10\beta$.

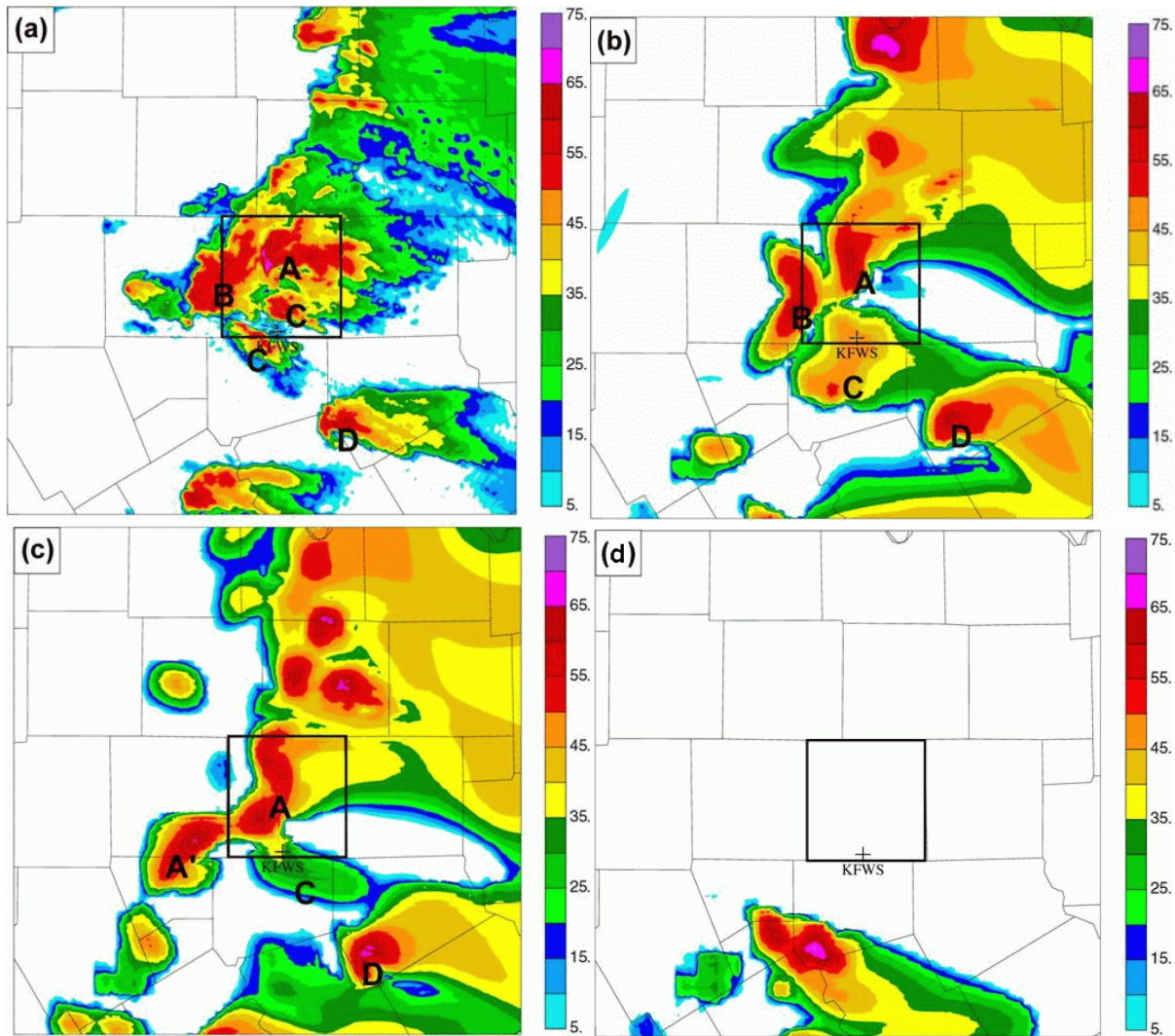


Fig 5. Fort Worth NEXRAD radar reflectivity image, 1.5 degree scan at 00:30 UTC, 29 Mar 2000. The domain shown here is 100 x 100 km. County boundaries are indicated with Tarrant County indicated in bold. Downtown Fort Worth is located in the center of Tarrant County. The location of the Fort Worth NEXRAD radar, KFWS, is indicated by the cross. See text for description of labelled storms.

4 Fort Worth Case Study

The 3DVAR and wind analysis were recently applied to a tornadic storm case, the Fort Worth tornado of 28 March 2000. In this case two significant tornadoes occurred in the Dallas-Fort Worth metropolitan area, one striking downtown Fort Worth and the other nearby Arlington, Texas. The tornado that struck Fort Worth caused significant damage to high-rise office buildings, killed two people, and injured 80 others.

The tornadic storm was one of a cluster of storms in North Texas that afternoon and evening. We

sought to test the data assimilation system on predicting the complex evolution of this group of storms, including the details of the storms' internal circulations.

This case was first used to test the ARPS Data Analysis System (ADAS, Brewster 1996, 2002), a Bratseth-method successive corrections approximation to optimal interpolation (Bratseth 1986), using the lower-precision NIDS radar data files. These results were reported in X03. Here we use the 3DVAR analysis method and the full-precision and complete-volume-scan data from the Level-II NEXRAD data files. Such complete data

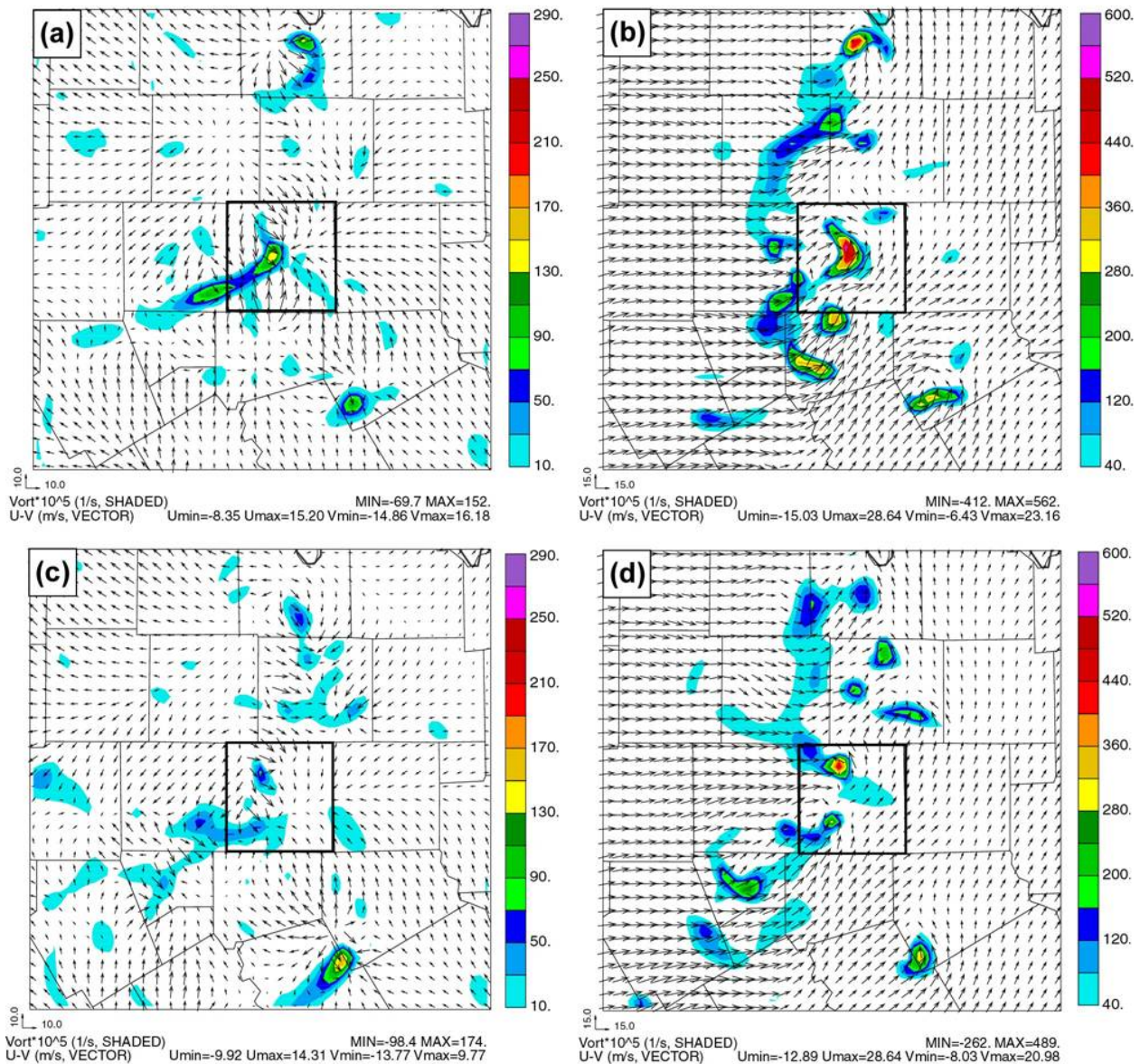


Fig 6. wind vectors and vertical vorticity for forecasts valid at 00:30 UTC on 30 Mar 2000, near the time of the first tornado in downtown Fort Worth. The frames in the left column (a,c) are valid at the first level above ground (10 m AGL) while the frames in the right column (b,d) show the fields at 3-km MSL. The upper panel (a,b) are forecasts made using reflectivity and velocity. The frames in the lower row are from forecasts made using just the reflectivity.

can now be obtained in real-time due to the recent upgrade to the NWS NEXRAD data distribution system as a result of the CRAFT project (Droegemeier et al. 2002). Complete details of this case are being prepared for formal publication in a two-part paper (Hu et al. 2005a,b).

A 9-km outer grid is run from an analysis at 1800 UTC, before thunderstorms had formed in the

area, and the data assimilation is done on a 3-km grid as an intermittent assimilation with 10-minute intervals during the hour 2200-2300 UTC. The forecast model is run forward from that time with no additional data input.

Figure 5a shows remapped radar reflectivity at 1.45° elevation from the Fort Worth radar (KFWS) as observed at 00:30 on March 29. The

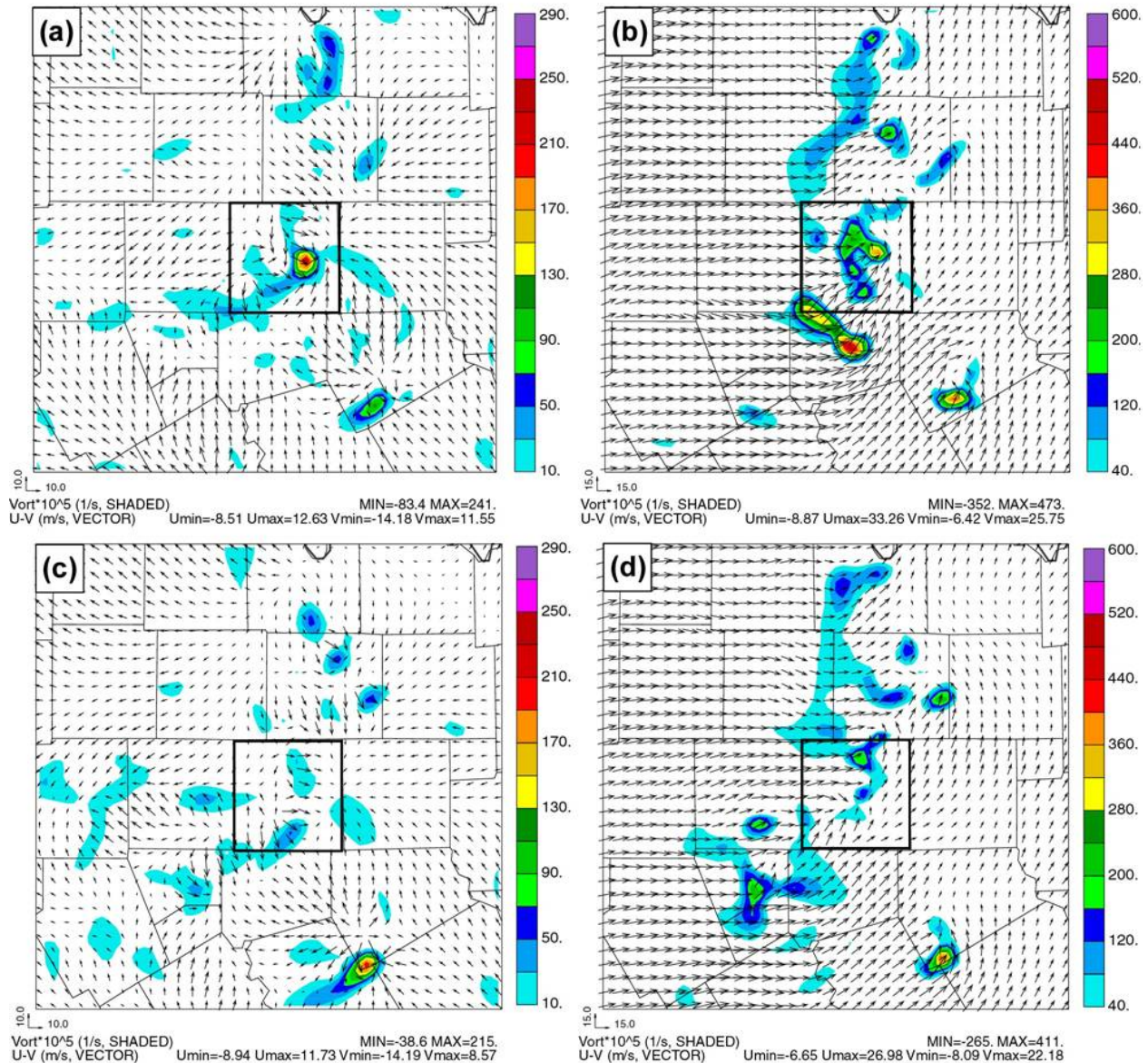


Fig 7. Forecast wind vectors and vertical vorticity valid at 00:45 UTC on 30 Mar 2000, near the edging time of the second tornado in Arlington. The frames in the left column (a,c) are valid at the first level above ground (10 m AGL) while the frames in the right column (b,d) show the fields at 3-km MSL. The upper panel (a,b) are forecasts made using reflectivity and velocity. The frames in the lower row are from forecasts made using just the reflectivity.

first tornado touched down in downtown Fort Worth at 00:15 and lasted until about 00:30. The radar at this time featured a cluster of storms (storms A, B, C, and C') in the Dallas-Fort Worth area. The cell marked A is the tornadic cell that struck downtown Fort Worth, after forming to the west of Tarrant County (outlined in bold in figure) and moving into the center of the county. Cell D is another supercell storm that

exhibited rotation and produced large hail. Figure 5b shows the 1.45° elevation angle radar reflectivity derived from the forecasted hydrometeors at 90 minutes into the forward forecast (150 minutes from the beginning of the data assimilation window). The forecast depicted in this frame used the radial wind data via the ARPS 3DVAR and the reflectivity via cloud analysis. The general positions of cells A, B and C are

similar to that observed, though C appears with two distinct cores in the observed reflectivity. Overall the patterns are smoother, but that is due in part to the 3 km resolution of the model

Figure 5c shows the same fields but from the forecast using only the reflectivity data in the cloud analysis, while Fig. 5d is the forecast that results from just using the radial wind analysis with no updates to the background forecast fields via the cloud and latent heat adjustment. The result for Fig 5c is quite similar to Fig 5b, demonstrating the strong impact of cloud and latent heat adjustments to the model forecast, while the forecast made by only assimilating the wind adjustments via 3DVAR is not able to create the significant storms of the day.

Similar results were found for the forecasts valid at the time of the second tornado, at 00:45. The forecast successfully shows cell mergers taking place among storms A, B, and C. Details are reported in Hu et al., 2005a,b.

Figure 6 shows the wind forecasts valid at the time of the first tornado in Fort Worth, with the vertical vorticity overlaid. The surface wind and the wind at 3-km are depicted in the figure in the left and right column, respectively, and the forecasts made using wind and reflectivity data are shown in the top row, with the reflectivity-only forecasts shown in the bottom row. The forecasts are successful in depicting strong vertical vorticity maximum near the location of the observed tornado at 3 km. The forecast using the radial wind shows stronger vertical vorticity at 3 km and in the surface wind.

Figure 7 is the same as Fig. 6, except at 00:45 UTC, near the time of the tornado at Arlington, Texas. As with the forecast at 00:30, the forecast at this time is able to produce strong rotation in the wind field near the location of the observed tornado.

4.1 Other Case Studies

Other successful case study simulations have been done using the ADAS scheme with radar data and the cloud analysis with the latent heat adjustment. Brewster (2002) reported on a successful two-hour long simulation from a single analysis near the time of storm initiation for one of the 3 May 1999 tornadic storms in Central Oklahoma.

Figure 8 shows the radar display for 2300 UTC compared to the result of a 1-h forecast. The shape and rotational characteristics of the storm are well forecasted, with an approximately 10-km displacement.

A case study showing utility of the ADAS analysis scheme in combination with the cloud analysis for pre-convective data assimilation is reported by Xue and Martin (2005). In that work the initiation of convection near a dryline was simulated using data from surface mesonets in a 9-3-1-km nesting configuration.

A case of an initialization of an ongoing MCS also showed an impact of the cloud analysis and diabatic adjustment process on short term forecasts of a mesoscale convective complex (MCS) in Oklahoma (Dawson and Xue 2005). In that work a 3-hour spin up was noted in the 3-km grid-scale forecasts when initialized from interpolated large-scale model forecasts. Adding just mesoscale surface information with the ADAS analysis resulted in a 1-hour reduction in the spin-up time. Adding the cloud analysis and diabatic heating completely eliminated the spin-up time.

5 Real-time Demonstrations

In addition to the case studies described, the modelling system has been run in real-time for several research field projects or demonstration campaigns. In addition a system utilizing the ADAS analysis is run daily and posted on the internet at URL <http://www.caps.ou.edu/wx>

The procedures have been automated using Perl scripts and have proven to be robust under a number of weather scenarios. Some of them are briefly described here.

5.1 IHOP

In the Spring of 2002 several universities, NCAR, NOAA and several international organizations collaborated on a field project focused on measuring water vapor and its impact on prediction of rainfall and thunderstorms (International H₂O Project, IHOP, Weckwerth et al. 2004). For the IHOP project CAPS ran ARPS with a 3-km grid spacing over a large part of the

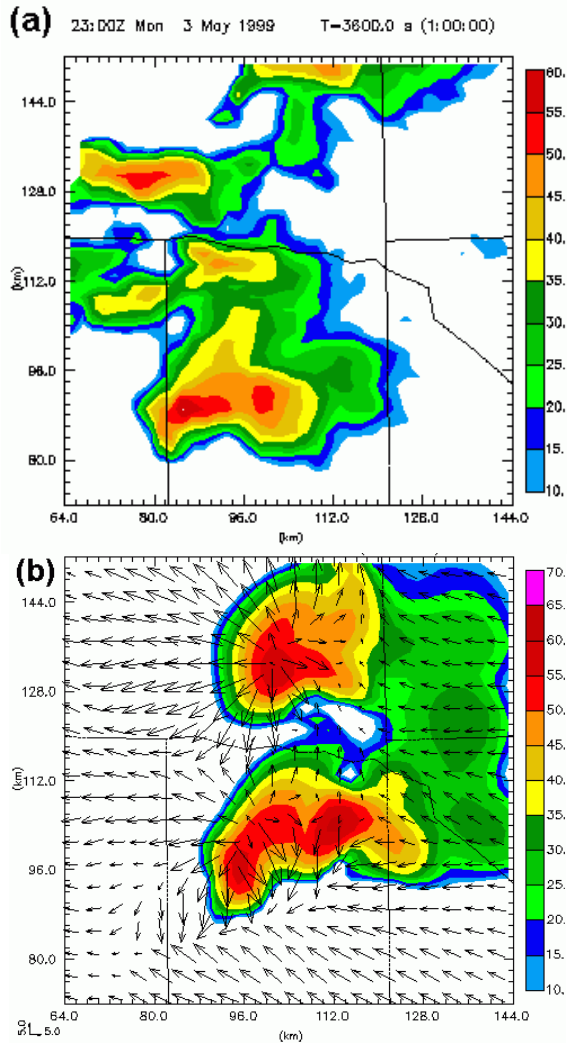


Fig 8. a) Observed radar reflectivity (dBZ) at 0.5 degree elevation from the KTLX radar 3 May 1999 2300 UTC. b) 1-h ARPS model forecast at 3-km grid resolution of radar reflectivity and wind at 10 m AGL valid at 2300 UTC.

Great Plains. This experiment used the ADAS with Bratseth analysis technique, the radial velocity and reflectivity data from a dozen radars in the Great Plains (Xue et al. 2002).

5.2 FAA Wintertime Test

For a six week period in the late fall and early winter of 2002 CAPS ran ARPS using the ADAS analysis with a 10-minute IAU in the Great Lakes region in of the assimilation system in wintertime conditions (Brewster et al. 2003). Data from several radars in the region were used in an analysis that was updated hourly.

The system was able to develop realistic fields of clouds and precipitation in the 10-min IAU window. Detection of icing conditions from the assimilated hydrometeors was as good as the best parameterized detection algorithm.

5.3 2004 SPC Spring Program

In the Spring of 2004 the ADAS Bratseth-based system was run at 4-km horizontal resolution over a large area of the central and eastern United States as part of the SPC/NSSL Spring Program (Weiss et al. 2004). The analyses produced for this area were converted to the format used by the Weather Research and Forecasting (WRF) model and numerical forecasts were made for 30 hour periods beginning at 00 UTC each evening. It is common to have significant convection occurring at that time of the data in the Great Plains and the forecasts demonstrated an ability to initialize and maintain such storms while other WRF model forecasts without the benefit of the analyses took 3 to 6 hours to spin-up the same convection.

Figure 9 is a sample forecast initialized at on 17 May 2004 00 UTC showing the 1-h precipitation between 00 and 01 UTC as observed by radar, the WRF forecast with CAPS' radar analysis and WRF forecast initialized with just interpolated fields from the Eta model. Note that the forecast initialized from an interpolation of a large-scale forecast produces very little precipitation even in areas with significant precipitation occurring while the CAPS-produced forecast with radar analysis initializes and maintains convection and non-convective precipitation in areas of strong synoptic and mesoscale forcing (Central and Northern Plains) and in areas of weak forcing (Alabama).

6 Conclusions and Future Work

A storm-scale 3DVAR and cloud analysis system for a non-hydrostatic NWP model, the ARPS, is described in this paper. The system and one using ADAS, a Bratseth-method successive correction analysis have been successfully applied to the seminal phase of a growing supercell thunderstorm, to predict the initiation of thunderstorms, and to a case of a cluster of existing thunderstorms consisting of storms at various stages of development. In the

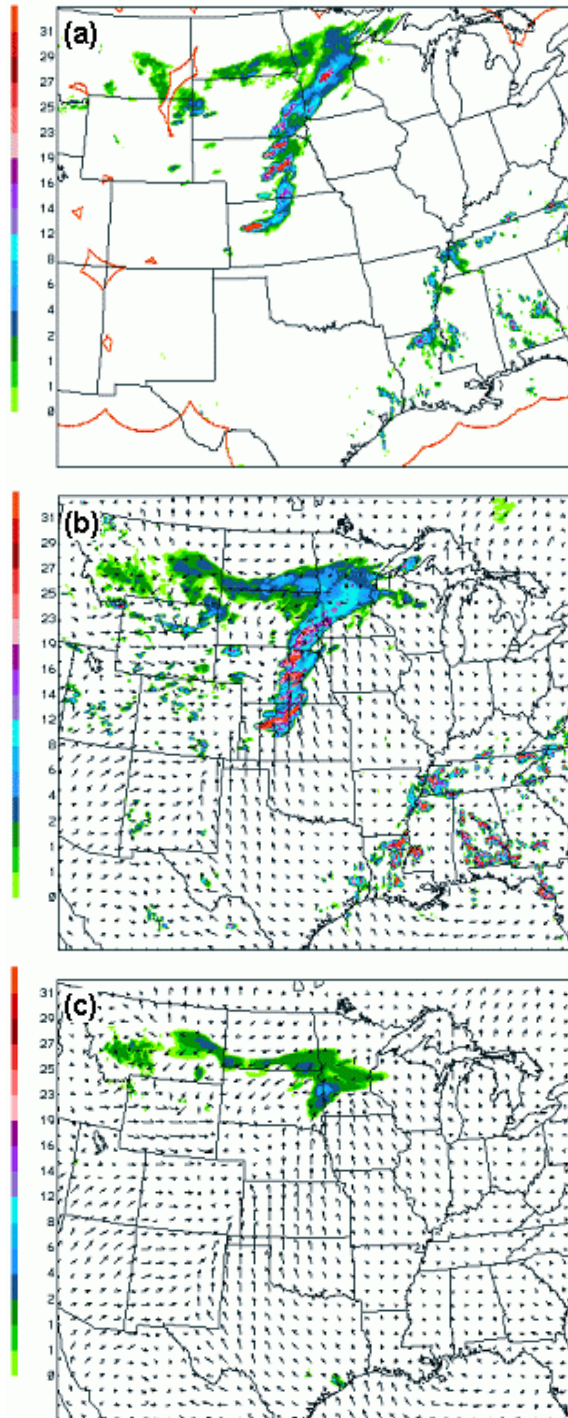


Fig 9. 1-hour accumulated precipitation from the 2004 SPC/NSSL Spring Forecasting exercise. A) observed rainfall from the NEXRAD radar network, Stage-II product, b) 1-h precipitation forecast WRF model initialized with ADAS including radar data, c) WRF model initialized from interpolated Eta model analysis.

latter case, with weak synoptic and mesoscale forcing, the Fort Worth tornadic storm of 28 March 2000 was successfully simulated using data from 1.5 hours before tornadogenesis. Data sensitivity studies have been done and demonstrate that the proper forecasting and maintenance of an existing thunderstorm is most sensitive to the diabatic adjustments that are applied based on the observed radar reflectivity. The formation of the mesocyclone is more accurately forecasted when radar radial velocity data are added using the 3DVAR technique, which includes a mass divergence constraint for coupling the wind components. In other cases with stronger synoptic or mesoscale forcing the diabatic adjustment is also important, though less crucial to producing a successful short-range forecast.

In addition to the case studies, the methods have demonstrated robustness. A similar system, using a Bratseth analysis in place of the 3DVAR analysis component was employed in a quasi-operational setting in cooperation with the Storm Prediction Center in the spring of 2004, for the 2002 IHOP field experiment, in a winter-time demonstration for the FAA, and in regular daily forecasts at CAPS. This system demonstrates notable improvement in short-range forecasts of convection over forecasts initialized with an interpolated field from larger-scale operational models.

Ongoing and future work includes parallelizing the Bratseth scheme-based ADAS code and later the 3DVAR code for more effective use on multiple-processor machines. We hope to conduct a real-time experiment utilizing the 3DVAR system to initialise the ARPS and/or WRF model and at a storm-resolving resolution over a significant portion of the United States perhaps as early as the spring of 2006.

7 Acknowledgments

The authors acknowledge the hard work and dedication of the many scientists and students who have contributed to the development of ARPS and the analysis tools. Dr. Daniel Weber, Kevin Thomas and Yungheng Wang have been instrumental in making the real-time operational model runs possible. The work is done under the capable leadership of Dr. Kelvin Droegemeier.

Preparation and presentation of this paper is supported by National Science Foundation (NSF) grant ATM-0331756 and the Sasaki Applied Meteorology Institute (SAMRI) at the University of Oklahoma (OU). Real-time Model runs were done on the facilities of the Pittsburgh Supercomputer Center (PSC) while others utilized the facilities of the Oklahoma Supercomputer Center for Education and Research (OSCER) at OU, PSC, and the National Center for Supercomputing Applications at the University of Illinois (NCSA).

Development of the analysis and assimilation tools and the research cited herein has been funded in part by the NSF through grants ATM-990907, ATM-0129892 and ATM-0331594 and by FAA through grant DOC-NOAA NA17RJ1227.

8 References

- Albers, S.C., J.A. McGinley, D.A. Birkenhuer, and J.R. Smart, 1996: The local analysis and Prediction System (LAPS): Analysis of clouds, precipitation and temperature. *Wea. and Forecasting*, **11**, 273-287.
- Bloom, S. C., L. L. Takacs, A. M. Da Silva, and D. Ledvina, 1996: Data assimilation using incremental analysis updates. *Mon. Wea. Rev.*, **124**, 1256-1271.
- Bratseth, A. M., 1986: Statistical interpolation by means of successive corrections. *Tellus*, **38A**, 439-447.
- Brewster, K., 1996: Application of a Bratseth analysis scheme including Doppler radar data. *Preprints, 15th Conf. on Wea. Analysis and Forecasting*. Amer. Meteor. Soc., 92-95.
- Brewster, K., 2002: Recent advances in the diabatic initialization of a non-hydrostatic numerical model. *Preprints, 21st Conf. on Severe Local Storms, and Preprints, 15th Conf. Num. Wea. Pred. and 19th Conf. Wea. Anal. Forecasting*, San Antonio, TX, Amer. Meteor. Soc., J51-54.
- Brewster, K., A. Shapiro, J. Gao, E. M. Kemp, P. Robinson, and K.W. Thomas, 2003: Assimilation of radar data for the detection of aviation weather hazards. *Preprints, 31st Conf. on Radar Meteorology*, Seattle, WA, Amer. Meteor. Soc., Boston, 118-121.
- Carpenter, R. L. J., K. K. Droegemeier, G. M. Bassett, S. S. Weygandt, D. E. Jahn, S. Stevenson, W. Qualley, and R. Strasser, 1999: Storm-scale numerical weather prediction for commercial and military aviation, Part I: Results from operational tests in 1998. Preprints, 8th Conf. on Aviation, Range, and Aerospace Meteor., Dallas, TX, Amer. Meteor. Soc., 209-211.
- Droegemeier, K.K., 1990: Toward a science of storm-scale prediction. Preprints, 16th conf. on Severe Local Storms, Kananaskis Park, Alberta, Canada, Amer. Meteor. Soc., 256-262.
- Droegemeier, K. K., M. Xue, A. Sathye, K. Brewster, G. Bassett, J. Zhang, Y. Liu, M. Zou, A. Crook, V. Wong, and R. Carpenter, 1996a: Real-time numerical prediction of storm-scale weather during VORTEX '95. Part I: Goals and methodology. Preprints, 18th Conf. on Severe Local Storms, San Francisco, CA, Amer. Meteor. Soc., 6-10.
- Droegemeier, K.K., M. Xue, K. Brewster, Y. Liu, S. Park, F. Carr, J. Mewes, J. Zong, A. Sathye, G. Bassett, M. Zou, R. Carpenter, D. McCarthy, D. Andra, P. Janish, R. Graham, S. Sanielvici, J. Brown, B. Loftis, and K. McLain, 1996b: The 1996 CAPS spring operational forecasting period: Real-time storm-scale NWP, Part I: Goals and methodology. Preprints, 11th Conf. on Num. Wea. Pred., Norfolk, VA, Amer. Meteor. Soc., 294-296.
- Droegemeier, K. K., 1997: The numerical prediction of thunderstorms: Challenges, potential benefits, and results from real time operational tests. *WMO Bulletin*, **46**, 324-336.
- Droegemeier, K. K., K. Kelleher, T. D. Crum, J. J. Levit, S. A. D. Greco, L. Miller, C. Sinclair, M. Benner, D.W. Fulker, and H. Edmon, 2002: Project CRAFT: A test bed for demonstrating the real time acquisition and archival of WSR-88D base (Level II) data. *Preprints, 18th Int. Conf. IIPS Meteor. Ocean. Hydrology*, Orlando, FL, Amer. Meteor. Soc., 136-139.
- Ferrier, B. S., 1994: A double-moment multiple-phase four-class bulk ice scheme. Part I: Description. *J. Atmos. Sci.*, **51**, 249-280.
- Gao, J., M. Xue, K. Brewster, F. Carr, and K. K. Droegemeier, 2002: New Development of a 3DVAR system for a non-hydrostatic NWP model. *Preprints, 15th Conf. Num. Wea. Pred. and 19th Conf. Wea. Anal. Forecasting*, San Antonio, TX, Amer. Meteor. Soc., 339-341.
- Gao, J.-D., M. Xue, K. Brewster, and K. K. Droegemeier, 2004: A three-dimensional variational data analysis method with recursive filter for Doppler radars. *J. Atmos. Ocean. Tech.*, **21**, 457-469.

- Gao, J., K. Brewster, and M. Xue 2005: A comparison of the radar ray path equations and approximations for use in radar data assimilation. *Adv. Atmos. Sci.*, Accepted
- Hu, M., M. Xue, and K. Brewster, 2005a: 3DVAR and Cloud Analysis with WSR-88D Level-II Data for the Prediction of Fort Worth Tornadoic Thunderstorms Part I: Cloud analysis. *Mon. Wea. Rev.*, Conditionally accepted.
- Hu, M., M. Xue, J.-D. Gao and K. Brewster: 2005b: 3DVAR and Cloud Analysis with WSR-88D Level-II Data for the Prediction of Fort Worth Tornadoic Thunderstorms Part II: Impact of radial velocity analysis via 3DVAR, *Mon Wea Rev.*, Conditionally accepted.
- Kessinger C., S. Ellis, J. VanAndel, D. Ferraro, and R. J. Keeler, 1999: *NEXRAD Data Quality Optimization, FY99 Annual Report*. Natl. Center for Atmospheric Research, Boulder, CO 80307.
- Lilly, D. K., 1990: Numerical prediction of thunderstorms - Has its time come? *Quart. J. Roy. Meteor. Soc.*, **116**, 779-798.
- Ren, D. and M. Xue, 2004: 4DVAR assimilation of ground temperature for the estimation of soil moisture and temperature.. Extended Abstracts, 20th Conf. Wea. Analysis & Forecasting/16th Conf. Num. Wea. Pred., Seattle, WA, Amer. Meteor. Soc.
- Smith, P. L., Jr., C. G. Myers, and H. D. Orville, 1975: Radar reflectivity factor calculations in numerical cloud models using bulk parameterization of precipitation processes. *J. Appl. Meteor.*, **14**, 1156-1165.
- Tong, M. and M. Xue, 2005: Ensemble Kalman filter assimilation of Doppler radar data with a compressible nonhydrostatic model: OSSE Experiments. *Mon. Wea. Rev.*, 1789-1807.
- Weckwerth, T.M., D. B. Parsons, S. E. Koch, J. A. Moore, M. A. LeMone, B. B. Demoz, C. Flamant, B. Geerts, J. Wang, and W. F. Feltz, 2004: An overview of the International H2O Project (IHOP_2002) and some preliminary highlights. *Bull. Amer. Meteor. Soc.*, **85**, 253-277.
- Weiss, S.J., J. S. Kain, J. J. Levit, M. E. Baldwin, and D. R. Bright, 2004: Examination of several different versions of the WRF model for the prediction of severe convective weather: The SPC/NSSL Spring Program 2004, *Extd Abstracts, 22nd Conference on Severe Local Storms*, Hyannis, MA., CD-ROM.
- Xue, M., K.K. Droegemeier, V. Wong, A. Shapiro, and K. Brewster, 1995: ARPS Version 4.0 User's Guide. 380pp [Available from Center for Analysis and Prediction of Storms, University of Oklahoma, Norman OK 73019]
- Xue, M., K. Brewster, K. K. Droegemeier, F. Carr, V. Wong, Y. Liu, A. Sathye, G. Bassett, P. Janish, J. Levit, and P. Bothwell, 1996a: Real-time numerical prediction of storm-scale weather during VORTEX-95. Part II: Operation summary and example cases. *Preprints: 18th Conf. on Severe Local Storms*, San Francisco, CA, Amer. Meteor. Soc., 178-182.
- Xue, M., K. Brewster, K. K. Droegemeier, V. Wong, D. H. Wang, F. Carr, A. Shapiro, L. M. Zhao, S. Weygandt, D. Andra, and P. Janish, 1996b: The 1996 CAPS spring operational forecasting period: Real-time storm-scale NWP, Part II: Operational summary and examples. *Preprints, 11th Conf. on Num. Wea. Pred.*, Norfolk, VA, Amer. Meteor. Soc., 297-300.
- Xue, M., Q. Xu, and K. K. Droegemeier, 1996b: A theoretical and numerical study of density currents in non-constant shear flows. Preprint, Seventh Conf. on Mesoscale Processes, Reading, UK, Amer. Meteor. Soc., 494-496.
- Xue, M., K. K. Droegemeier, and V. Wong, 2000: The Advanced Regional Prediction System (ARPS) - A multiscale nonhydrostatic atmospheric simulation and prediction tool. Part I: Model dynamics and verification. *Meteor. Atmos. Physics*. **75**, 161-193.
- Xue, M., K. K. Droegemeier, V. Wong, A. Shapiro, K. Brewster, F. Carr, D. Weber, Y. Liu, and D.-H. Wang, 2001: The Advanced Regional Prediction System (ARPS) - A multiscale nonhydrostatic atmospheric simulation and prediction tool. Part II: Model physics and applications. *Meteor. Atmos. Physics*. **76**, 143-165.
- Xue, M., K. Brewster, D. Weber, K. W. Thomas, F. Kong, and E. Kemp, 2002: Real-time storm-scale forecast support for IHOP 2002 at CAPS. *Preprints, 15th Conf. Num. Wea. Pred. and 19th Conf. Wea. Analysis Forecasting*, San Antonio, TX, Amer. Meteor. Soc.
- Xue, M., D.-H. Wang, J.-D. Gao, K. Brewster, and K. K. Droegemeier, 2003: The Advanced Regional Prediction System (ARPS), storm-scale numerical weather prediction and data assimilation. *Meteor. Atmos. Physics*, **82**, 139-170.
- Xue, M., M. Tong, and K. K. Droegemeier, 2005: An OSSE framework based on the ensemble

square-root Kalman filter for evaluating impact of data from radar networks on thunderstorm analysis and forecast. *J. Atmos. Ocean Tech.*, Accepted.

Xue, M., M. Tong, and K. K. Droegemeier, 2005: Impact of radar configuration and scan strategy on assimilation of radar data using ensemble Kalman filter. *9th Symp. Integrated Observing Assimilation Systems Atmosphere, Oceans, Land Surface*, Amer. Meteor. Soc., CDROM, 9.3.

Xue, M. and W. Martin, 2005: A high-resolution modeling study of the 24 May 2002 case during IHOP. Part I: Numerical simulation and general evolution of the dryline and convection. *Mon. Wea. Rev.*, Accepted.

Zhang, J., F. Carr and K. Brewster, 1998: ADAS cloud analysis. *Preprints, 12th Conf. on Num. Wea. Prediction*, Phoenix, AZ, Amer. Meteor. Soc., Boston, 185-188.